Estuaries and Coasts (2009) 32:54–67
DOI 10.1007/s12237-008-9112-1

Residual Exchange Flows in Subtropical Estuaries

Arnoldo Valle-Levinson · Guillermo Gutierrez de Velasco · Armando Trasviña · Alejandro J. Souza · Reginaldo Durazo · Ashish J. Mehta

Received: 9 June 2008 / Revised: 11 August 2008 / Accepted: 10 October 2008 / Published online: 5 November 2008

Abstract Observations of residual exchange flows at the entrance to four subtropical estuaries, two of them semiarid, indicate that these flows are mainly tidally driven, as they compare favorably with theoretical patterns of tidal residual flows. In every estuary examined, the tidal behavior was that of a standing or near-standing wave, i.e., tidal elevation and tidal currents were nearly in quadrature. The pattern of exchange flow that persisted at every estuary exhibited inflow in the channel and outflow over the shoals. Curiously, but also fortuitously, this pattern coincides with the exchange pattern driven by density gradients in other estuaries. The tidal stresses and the residual elevation slopes should be the dominant mechanisms that drive such tidal residual pattern because the Stokes transport mechanism is negligible for standing or near-standing waves. Time series measurements from the semiarid estuaries showed fortnightly modulation of the residual flow by tidal forcing in such a way that the strongest net exchange flows developed with the largest tidal distortions, i.e., during spring tides. This modulation is opposite to the modulation that typically results in temperate estuaries, where the strongest net exchange flows tend to develop during neap tides. The fortnightly modulation on tidal residual currents could be inferred from previous theoretical results because residual currents arise from tidal distortions but is made explicit in this study. The findings advanced herein should allow the drawing of generalities about exchange flow patterns in subtropical estuaries where residual flows are mainly driven by tides.

Keywords Tidal residuals · Subtropical estuaries · Exchange flows

A. Valle-Levinson (✉) · A. J. Mehta
Civil and Coastal Engineering Department, University of Florida, Gainesville, FL 32611, USA
e-mail: arnoldo@ufl.edu

G. Gutierrez de Velasco · A. Trasviña
Centro de Investigación Científica y Educación Superior de Ensenada,
La Paz, Baja California Sur, Mexico

A. J. Souza
Proudman Oceanographic Laboratory,
6 Brownlow Street,
Liverpool L3 5DA, UK

R. Durazo
Universidad Autonoma de Baja California,
Ensenada, Baja California, Mexico

Introduction

Subtropical estuaries, in the context of this study, are those semi-enclosed bodies of water found poleward of the Tropics of Cancer (~23.5° N) and Capricorn (~23.5° S) but equatorward of ~30° N and 30° S. These latitude bands receive less precipitation than the tropical and temperate latitudes because of the dominant high atmospheric pressure systems associated with the transition between the trade winds and the westerlies (e.g., Pinet 2006). Therefore, when winds are moderate to weak, most estuaries in the subtropical latitude band are mainly forced by tides because freshwater input is negligible or sporadic. This tidal forcing, in itself, can produce residual currents through nonlinear interactions with bathymetry (e.g., Pingree and Maddock 1977; Zimmerman 1978). Such interactions with bathymetry, and also morphology, may be examined through vorticity tendencies to explain the mechanisms that generate the tidal residuals (Robinson 1981).

Recent theoretical findings indicate that the pattern of tidal residuals is greatly influenced by channel-shoals bathymetry (Li and O'Donnell 2005; Winant 2008). The tidal residual exchange pattern depends on whether the tide is progressive (in a long basin) or standing (in a short

basin). For standing tidal waves, the exchange pattern at the basin's entrance results from an inner pair of gyres with net inflow in the channel and outflow over the adjacent shoals (Fig. 1). The exchange pattern in basins with progressive tidal waves displays inner and outer pairs of gyres. At the basin's entrance, the pattern results in net outflow in the channel and inflow over shoals (Fig. 1). In the vertically integrated view of Li and O'Donnell (2005), flow does not cross the boundary between inner and outer gyres. In the local view (Fig. 9 in Winant 2008), fluid parcels cross the boundary, i.e., the inner gyre is not isolated from the ocean. In subtropical estuaries, the net exchange flow at the entrance is then expected to reveal one of these patterns.

The purpose of this study is to present observational evidence that supports the theoretical results of Li and O'Donnell (2005) and Winant (2008) for tidal residuals in homogeneous (or well-mixed) systems. Observational evidence is presented from different systems located in major (>600 km long) peninsulas: two systems in Florida and two in the Baja California peninsula in Mexico (Fig. 2). The two systems in Florida, Saint Augustine Inlet and Jupiter Inlet, are on the east coast of the peninsula and are separated by ~350 km. The two lagoons in Mexico are semiarid (evaporation exceeds precipitation through an annual cycle), separated by a distance of ~900 km and are on both sides of the Baja California peninsula. One lagoon, San Quintin Bay, connects to the Pacific Ocean, and the other lagoon, Ensenada de La Paz, is linked to the Gulf of California through the Bay of La Paz. All of the systems discussed in this paper are characterized by sporadic freshwater inputs that are believed to influence their hydrodynamics only transiently. Therefore, the embayments featured in this study are forced mainly by tides and intermittently by wind. Because of their overall weak to negligible water column stratification and their predominant forcing by tides, these embayments represent ideal natural laboratories where theoretical ideas on tidal residual flows can be tested.

This paper is organized as follows. Recent theoretical considerations on tidal residual flows affected by bathymetry are reviewed briefly. Then, the data sources that are compared to theory are described. The spatial structure of the residual flows observed at the four embayments is presented next. The paper continues with a discussion on the potential generality of these observations and on the resemblance of the tidally induced exchange pattern to that produced by other forcings. The paper concludes with the main findings.

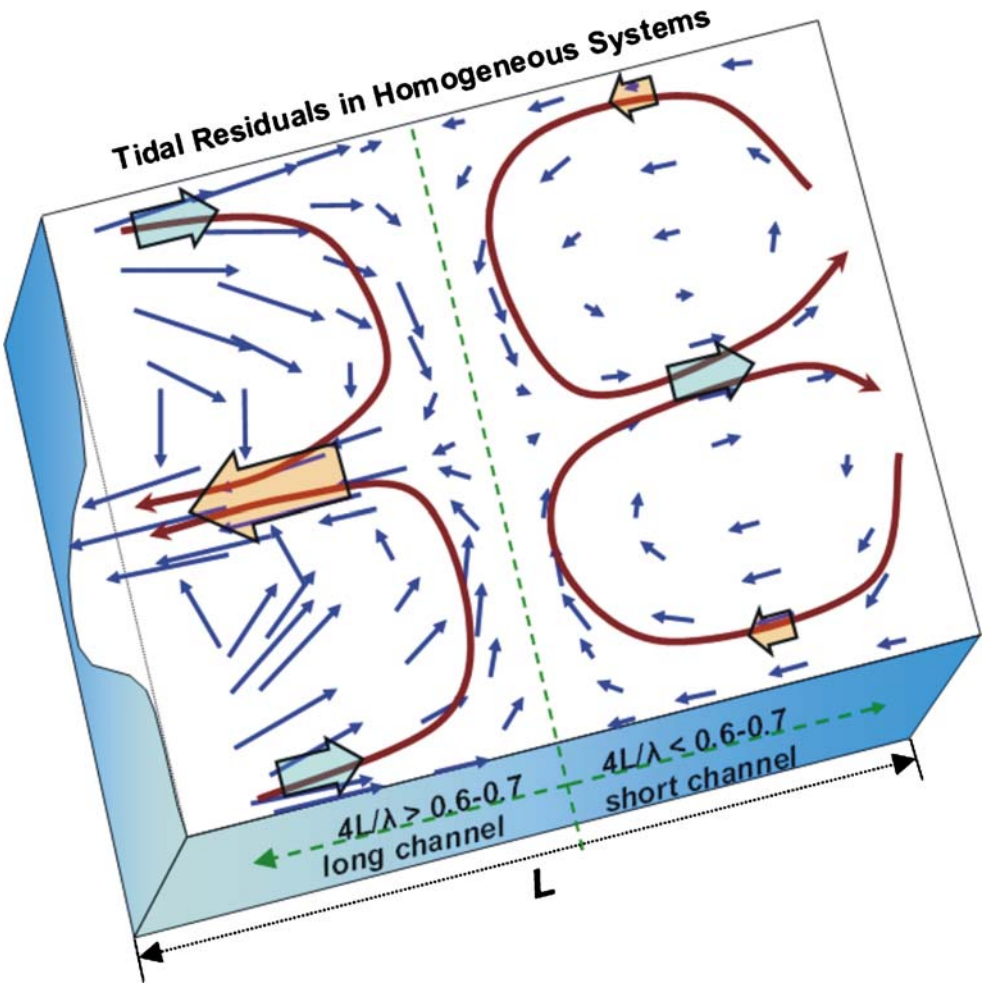

Fig. 1 Schematic of depth-averaged tidal residual flow derived from theoretical results of Li and O'Donnell (2005) and Winant (2008). The parameter λ indicates the tidal wavelength

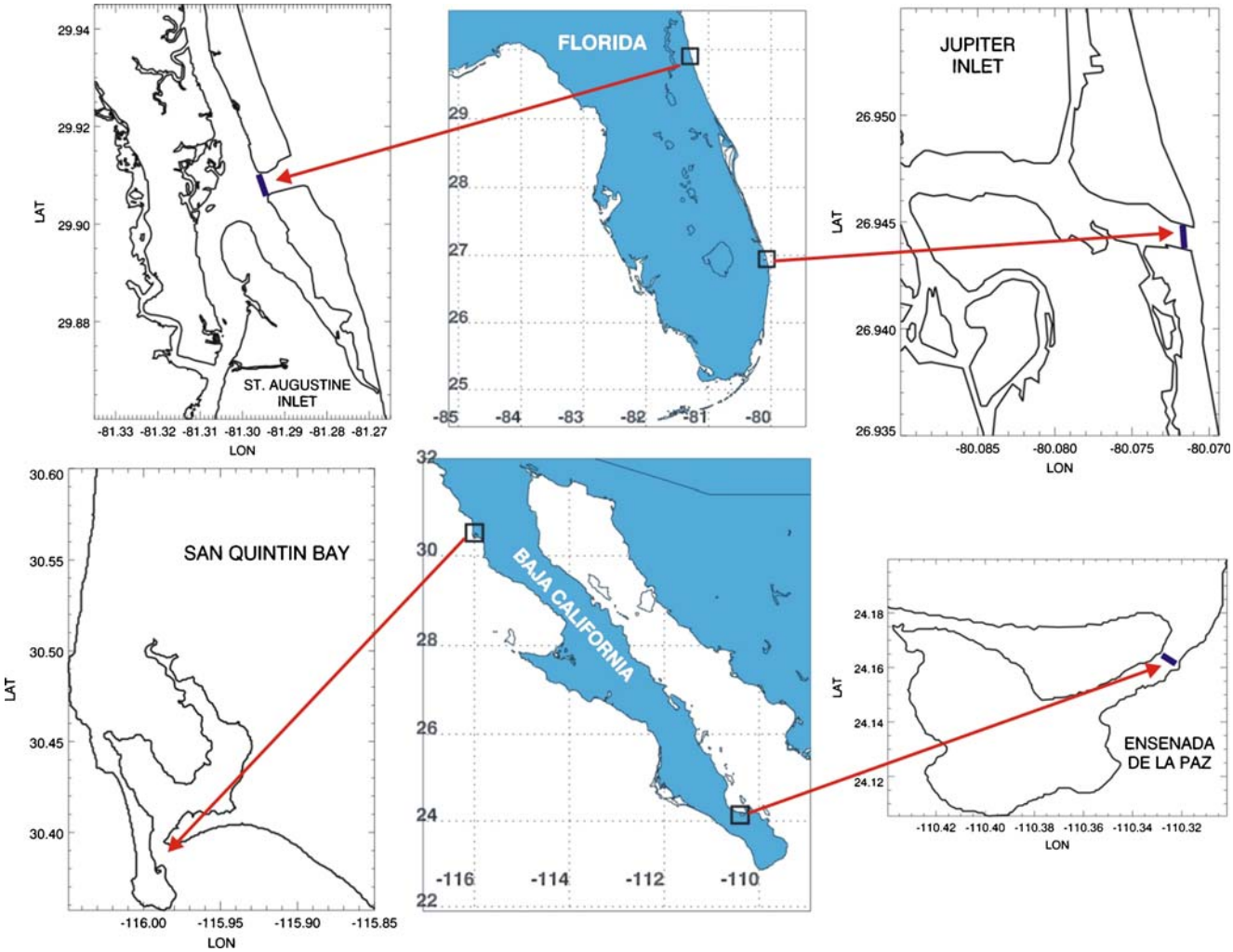

Fig. 2 *Upper panels*, from *left to right*, show Saint Augustine Inlet, the Florida peninsula and Jupiter Inlet. *Lower panels* show San Quintin Bay, the Baja California peninsula and Ensenada de La Paz

Brief Review of the Theory

The arguments presented by Li and O'Donnell (2005) for basins with uniform along-basin channel-shoals bathymetry are followed in this section. They use a perturbation method in which the solution is assumed to be a superposition of the first (or lowest), second, and higher order contributions to the flow. A linear solution is obtained for the lowest order, vertically averaged tidal flow U_1, V_1, where U and V are the along-basin and cross basin depth-averaged flows (m/s), respectively. The subscript 1 indicates lowest order or tidal fields. These tidal fields are used to obtain the following order, tidally averaged (U_T, V_T), solutions:

$$U_T = 2\underbrace{\left\langle \frac{U_1\eta_1}{H} \right\rangle}_{\mathrm{I}} - \underbrace{\frac{H}{r}\left(\left\langle U_1 \frac{\partial U_1}{\partial x} \right\rangle + \left\langle V_1 \frac{\partial U_1}{\partial y} \right\rangle \right)}_{\mathrm{II}} - \underbrace{\frac{gH}{r}\left\langle \frac{\partial \eta_2}{\partial x} \right\rangle}_{\mathrm{III}}$$

$$V_T = 2\underbrace{\left\langle \frac{V_1\eta_1}{H} \right\rangle}_{\mathrm{I}} - \underbrace{\frac{H}{r}\left(\underbrace{\left\langle U_1 \frac{\partial V_1}{\partial x} \right\rangle}_{\mathrm{a}} + \underbrace{\left\langle V_1 \frac{\partial V_1}{\partial y} \right\rangle}_{\mathrm{b}} \right)}_{\mathrm{II}} - \underbrace{\frac{gH}{r}\left\langle \frac{\partial \eta_2}{\partial y} \right\rangle}_{\mathrm{III}} \quad (1)$$

where the brackets < > denote tidal averages, g is the acceleration due to gravity (9.8 m/s^2), H is the water depth (m), η_1 is the tidal amplitude (m), η_2 is the residual sea surface elevation (m), and r is a linearized bottom drag coefficient (in m/s) that depends on the tidal current amplitude U_o and equals $8C_d \cdot U_o/3\pi$; C_d is a non-dimensional drag coefficient (0.0025). The tidal residual flows (left-hand side of Eq. 1) are driven by three processes: Terms I on the right-hand side (rhs) of 1 are related to the tidally averaged covariance between tidal elevation and tidal currents, i.e., the Stokes velocity; terms II represent residual flows produced by horizontal gradients (divergences by terms II-a and lateral shears by terms II-b) in tidal velocities, these terms are sometimes called Reynolds stress (e.g. Winant 2008) or tidal stress (e.g. Nihoul and Ronday 1975); and terms *III* are related to flows produced by residual (higher order) sea level slopes. All of these terms become relevant for the residual flow in basins where the ratio of the tidal amplitude to water depth is relatively large, i.e., $\eta_1/H>0.1$. Winant (2008) adds three-dimensionality to the problem by allowing Earth's rotation and depth-dependent flows as part of the solution. The essence of Li and O'Donnell's solution remains unaltered, relative to Winant's, for systems like those considered in this study where Earth's rotation effects are negligible. This is because the vertically integrated flows of Li and O'Donnell's solution are equivalent to the transport stream function of Winant's solution.

Over laterally varying bathymetry, the exchange pattern at the entrance to the basin is opposite from long to short basins (Li and O'Donnell 2005). In addition, the exchange pattern at the entrance to basins with weak frictional effects is opposite to the pattern that develops under moderate to strong friction (Winant 2008). The patterns that arise in long channels are similar to the patterns under moderate to strong friction. A long basin is considered to have a length L greater than one fourth of the tidal wavelength λ times 0.6, i.e., $L>0.6\lambda/4$ (Fig. 1; Li and O'Donnell 2005). Moderately to strongly frictional basins are those where the amplitude of the oscillatory bottom boundary layer occupies more than ~30% of the water column (Winant 2008). Regardless of whether the channel is long or short, terms II in Eq. 1 produce net flows (vertically integrated) into the basin and terms III in Eq. 1 induce net flows out of the basin across the entire basin (Li and O'Donnell 2005; Winant 2008). The Stokes velocity (terms I) is the mechanism that ultimately determines whether the net flow in the channel and over the shoals, is out of or into the basin. This is because, in short channels, the tide is a standing wave and the tidal elevation and currents are in quadrature, making the Stokes velocity tend to zero. In long basins, the Stokes velocity is inward throughout the basin's cross-section but is strongest over the shoals, where H is minimum. This Stokes velocity, interacting with the stress and residual slope velocities in long basins, causes a pattern of net inflow over shoals and outflow in the channel at the basin's entrance. The absence of the Stokes velocity in short basins causes the opposite pattern of inflow in channel and outflow over shoals, as observed at the entrance to all systems portrayed in this paper.

Observations from four short systems were placed in the context of the above theoretical ideas. An important commonality in all four systems is that they display standing or near-standing tidal wave conditions. This indicates that tidal currents and water level are close to 90° out of phase or in quadrature. Consequently, the Stokes drift mechanism for generation of tidal residual currents should be negligible, and all four systems should exhibit 'short' basin characteristics (Li and O'Donnell 2005; Winant 2008). This means that the tidal residual currents should display inflow, from surface to bottom (or vertically integrated), in the channel and outflow (also throughout the water column or vertically integrated) over the shallower shoals. It is hypothesized that because such a pattern results from tidal forcing, it should display a fortnightly modulation consisting of stronger exchange flows during spring tides than during neap tides. The data from the Florida peninsula are used to compare with the spatial structure of exchange flows predicted from theory. The data from the Baja California peninsula provide information to test the hypothesis by examining the tidal modulation of exchange flows.

Data Sources

The data presented in this work consist of current velocity profiles obtained with acoustic Doppler current profilers (ADCPs). The data from the two Florida embayments were collected at the entrance to inlets during semidiurnal tidal-cycle (~12 h) surveys. The data from Ensenada de la Paz were obtained at the entrance to the lagoon on 24-h surveys during spring and neap tides and from an ADCP that was moored for 60 days. The data from San Quintin Bay were obtained from an ADCP that was moored for 30 days.

Data from Saint Augustine Inlet were recorded underway on February 2, 2006 with a boat-mounted 1,228.8-kHz ADCP at 1-s pings, 0.5-m vertical bins, and averaged every 15 m in the horizontal. The data collection and processing, as well as the results of that experiment, have been described in detail in Webb et al. (2007). Data from Jupiter Inlet were obtained underway in the period between 12:00 GMT and 23:30 GMT on May 9, 2006 with a boat-mounted 1,228.8-kHz ADCP. Velocity data were recorded at 1-s pings with vertical bins of 0.5 m and averaged over 5 m in the horizontal. In Ensenada de La Paz survey, data were also collected underway during spring tides from 15:15 GMT on July 21, 2002 until 15:30 GMT on July 22, 2002

Table 1 Characteristics of lagoons studied

	H (m)	L (km)	λ_{M2} (km)	4 L/λ_{M2}
St Augustine Inlet	5	30	313	0.38
Jupiter Inlet	3	20	242	0.33
Ensenada de la Paz	4	12	280	0.17
San Quintin Bay	3	12	242	0.20

The semidiurnal tidal wavelength is given by λ_{M2}. Values of depth H represent approximate averages for the entire systems, not only the entrance.

and during neap tides from 14:37 GMT on July 28, 2002 to 15:22 GMT on July 29, 2002. On that occasion, a boat-mounted 614.4 kHz ADCP was used to collect data every 0.7 s at 0.5-m bins and averaged over 10 m in the horizontal. Furthermore, a 60-day time series of velocity profiles was recorded with a bottom-mounted 307.2-kHz ADCP that was deployed at a depth of 6 m from March 11, 2003 to May 5, 2003. Data were recorded at 25-min intervals and 0.5-m bins. Finally, in San Quintin Bay, a bottom-mounted 1228.8-kHz ADCP was deployed in the middle of the channel at the entrance to the lagoon at a depth of 13 m. Data were collected every 10 min at 0.5-m bins from May 21, 2004 to June 16, 2004. The main characteristics of the four basins examined are given in Table 1.

Exchange Flows

In this section, the spatial pattern of tidal residual flows, the local circulation (Winant 2008), is first explored with tidal-cycle survey data in Saint Augustine and Jupiter inlets. The tidal properties at both Florida inlets are similar even though the tidal range is ~1.5 m at Saint Augustine and ~0.75 m at Jupiter inlet. The tide is predominantly semidiurnal at both locations. In addition, because the mean depth at Saint Augustine is almost twice as large as that at Jupiter (Table 1), the ratio of tidal amplitude η to water depth H, a measure of tidal nonlinearities (Parker 2007), is ~0.1–0.2 at both inlets. In addition, the tidal currents and elevation are close to 3 h out of phase, i.e., near quadrature, at both inlets. Wind forcing played a negligible role on the flow patterns observed.

The spatial pattern of residual flows is also explored at the entrance to Ensenada de la Paz as well as the variation of this pattern from spring to neap tides. The long-term modulation of the residual flows in these semiarid lagoons is explored with time series at the entrance to both Ensenada de La Paz and San Quintin Bay. Both lagoons in the Baja California peninsula have mixed tides with tidal ranges in Ensenada de La Paz that oscillate from 0.75 m in neap tides to 1.5 m in spring tides. In San Quintin, the tidal range is 1.5 m in neap tides and 2.5 m in spring tides. Mean depths are 6 and 12 m at the entrance to La Paz and San Quintin, respectively, and the ratio η/H in these two systems is >0.1 and appreciable tidal distortion is observed. The tidal currents and elevation are in quadrature at both lagoons.

In Saint Augustine Inlet, 13 transect repetitions during a semidiurnal tidal cycle were used to calculate tidally averaged flows through a least squares fit to mean flows plus semidiurnal and quarterdiurnal harmonics (e.g., Valle-Levinson and Atkinson 1999). Buoyancy input and horizontal density gradients during the day of the experiment were negligible compared to tidal forcing (Webb et al. 2007). The tidally averaged along-inlet flows exhibited a clear bathymetric partition (Fig. 3a) with net inflows in the channel and outflows over the shoals. Net volume inflow was 190 m^3/s and net outflow was 210 m^3/s. The flow pattern could be attributed to either density-driven flow under high frictional effects (e.g., Wong 2004; Valle-Levinson 2008) or to tidally driven flows in a short channel (Li and O'Donnell 2005). Clearly, the flow pattern was not driven by density gradients (Webb et al. 2007) and was caused by the rectification, or distortion, of the tidal currents through non-linear effects (as described in Eq. 1). From the three mechanisms driving the tidal residual flows, the Stokes velocity (terms I in Eq. 1) should have been negligible because of the observed standing wave. The residual slope terms (terms III in Eq. 1) could not be evaluated with the data available. Only part of the stress terms (terms II-b) was quantifiable with the data collected (Fig. 3b). In order to be consistent with theory, the stress terms (terms II) should have been negative, i.e., into the basin, throughout the transect measured. The contribution from the lateral shear (term II-b) was negative almost across the entire transect (Fig. 3b). However, the magnitude of II-b indicated a production of excessively large U_T (Fig. 3b). This implied that the contribution to term II related to flow divergence (term II-a) would also have to be very large to counteract the shear magnitude and produce a reasonable net flow. As suggested by Webb et al. (2007), the pattern of exchange flows observed in Saint Augustine inlet was caused by nonlinearities from bottom friction and from advective accelerations.

The survey at Jupiter Inlet produced 21 repetitions of the cross-inlet transect. This inlet, only 80 m wide and 5 m deep, is influenced by Gulf Stream waters (salinity of 36.5) during flood and slightly lower salinity water (35) during ebb (Fig. 4). The tidally averaged horizontal density gradient $<\partial\rho/\partial x>$ was estimated with data from three CTD stations located along the inlet and sampled ten times throughout the tidal cycle. The value of $<\partial\rho/\partial x>$ was O (10^{-4}) kg/m^4, which is comparable to estuaries where the nontidal circulation is driven by density gradients (e.g., the Hudson River, Geyer et al. 2000). However, the tidally

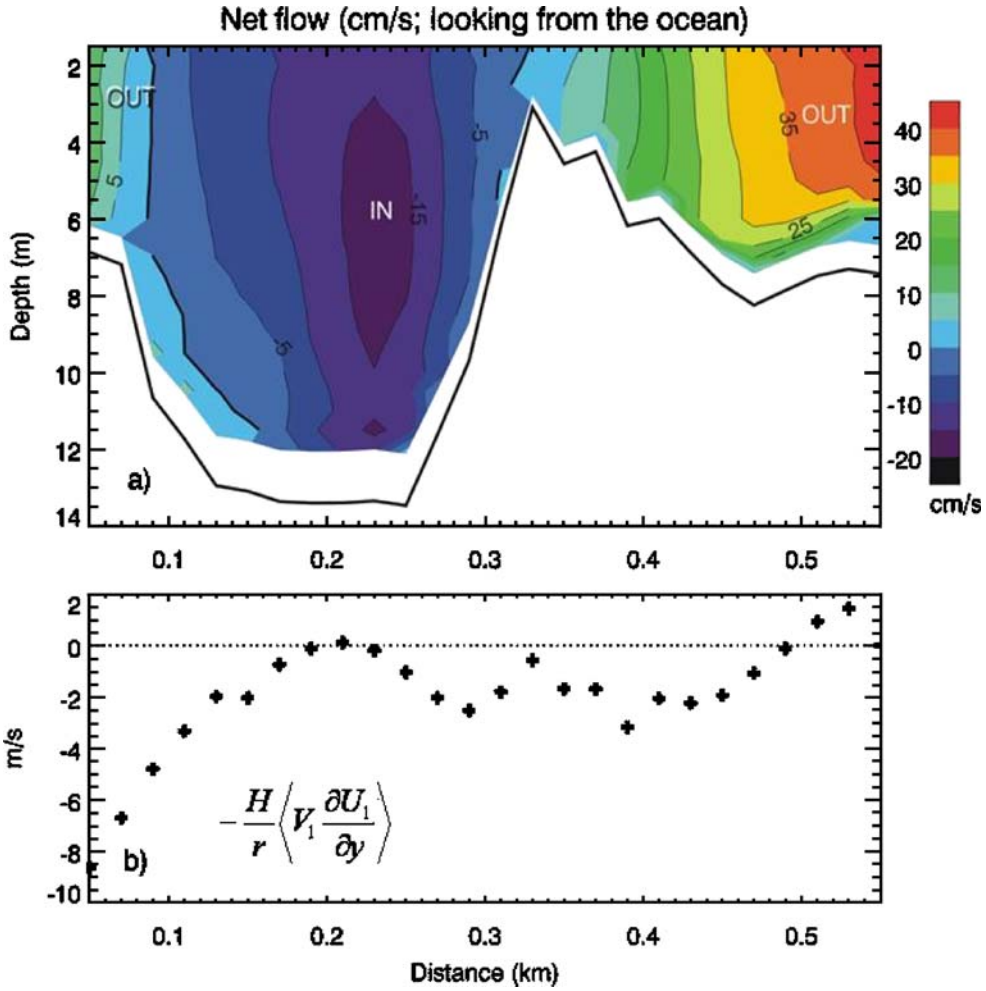

Fig. 3 Net exchange flow at the entrance to Saint Augustine Inlet (**a**) and contribution to the stress-induced tidal residual flow (term II-b of Eq. 1) by the lateral shears in the tidal currents across the sampling transect (**b**)

averaged accelerations produced by the baroclinic pressure gradient $\langle (gH/\rho)\ \partial\rho/\partial x \rangle$ at Jupiter Inlet were of O(10^{-6}) m/s^2 because of its shallow depths (H<5 m). These accelerations were two orders of magnitude smaller, for instance, than those arising from the tidally averaged bottom stresses $\langle C_d\ u\ (u^2+v^2)^{1/2}/H \rangle$, which were O($10^{-4}$) m/s^2. Therefore, the pattern of net inflow in the middle of the section and outflow over the sides (Fig. 4a) was most likely driven by tidal distortion. In this case, the net volume outflow was 4 m^3/s and the net inflow was 8 m^3/s. The flow pattern was consistent with theoretical results for a short basin where the tide is a standing wave. The residual flow arising from stress terms (terms II in Eq. 1) should be directed into the basin throughout the cross-section. This was nearly the case, as it was in Saint Augustine Inlet, for the exclusive contribution from the lateral shear (term II-b), the only quantifiable term in Eq. 1 with the data available (Fig. 4b). The magnitude of the residual flow U_T produced by this term was still high but closer (0.6 vs. 0.1 m/s) to the values of residual currents observed, which indicates less influence of lateral shear and divergence than in Saint Augustine Inlet. Two questions arise from these observed patterns of tidally averaged flows at the two Florida inlets: (1) How persistent are these patterns from day to day and week to week, and (2) are these patterns modulated by tidal forcing (spring versus neap)? The answer to these questions is addressed with the data collected at the embayments on the Baja California peninsula.

The surveys at the entrance to Ensenada de la Paz consisted of 33 repetitions during spring tides and 31 during neap tides. These surveys extended throughout a diurnal cycle to cover the mixed diurnal character of the tide. During the surveys, net evaporation losses, which are typical of summer months in that region of the Baja California peninsula, caused the lagoon to be hypersaline with a mean salinity >35.7. The values of $\langle \partial\rho/\partial x \rangle$ were similar to those in Jupiter Inlet (O(10^{-4} kg/m^4)), which also made the values of $\langle (gH/\rho)\ \partial\rho/\partial x \rangle$ of O(10^{-6}) m/s^2. These gradients changed insignificantly from neap to spring tides. As with Jupiter Inlet, values of $\langle C_d\ u\ (u^2+v^2)^{1/2}/H \rangle$ were of O(10^{-4}) m/s^2 causing the mean flow to be driven by tidal distortions and not by density gradients nor by wind stress, which was insignificant during both surveys.

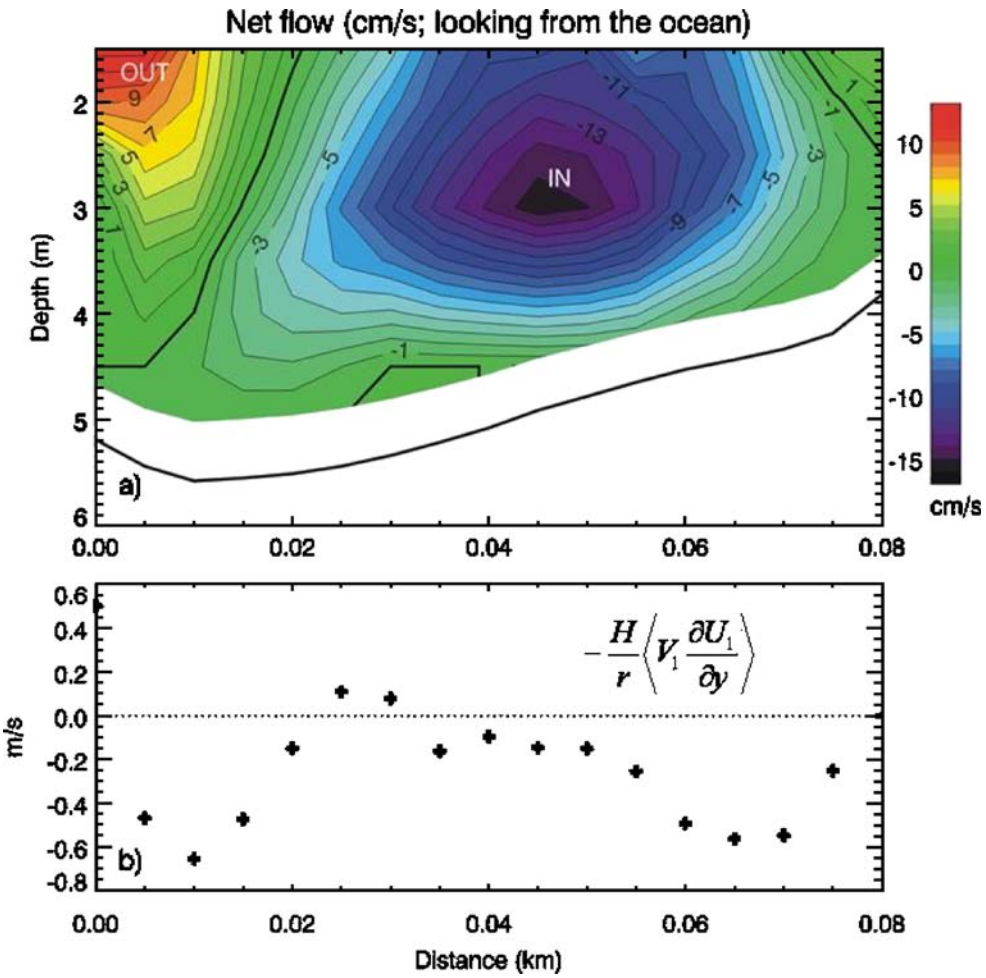

Fig. 4 Same as Fig. 3 but for Jupiter inlet

The bathymetry at the entrance to Ensenada de la Paz is peculiar in the sense that it displays two channels, rather than one, with a deeper channel to the south (to the left on Fig. 5a). The difference in depth between the two channels is crucial to determine the location of tidally averaged inflows and outflows because the stress terms (terms II in Eq. 1) are proportional to depth. Unidirectional net inflows appeared in the deeper channel, and net outflows developed in the shallower channel (Fig. 5a). The lateral shear mechanism (term II-b, shown in Fig. 5b) produced net currents that were of similar magnitude to those observed. The spatial distribution of term II should have been negative (into the basin) throughout the transect in order to account for the stress mechanism. Because term II-b changed sign across the transect, the flow divergence influence (term II-a) should have contributed for term II to become negative throughout the transect. It is noteworthy that the contribution from the stress term (*II* in Eq. 1) was typically one order of magnitude smaller in Ensenada de la Paz than at the Florida systems. The reduced magnitude of term II-b in Ensenada de la Paz was likely the result of much sharper bathymetric gradients across the transect in Saint Augustine Inlet, which induced larger lateral shear in the tidal and residual currents.

The net exchange pattern, the local circulation (Winant 2008), at the entrance to Ensenada de la Paz was qualitatively consistent from spring to neap tides, but the net flows were stronger during spring tides than during neap tides. During spring tides, maximum inflow was >10 cm/s and the strongest outflow was ~7 cm/s (Fig. 5a). In contrast, during neap tides, inflows were <5 cm/s and outflows only <2 cm/s (Fig. 6a). Net volume outflow was 55 m^3/s, and net inflow was 50 m^3/s during spring tides. In neap tides, volume inflow was 15 m^3/s, and outflow was 13 m^3/s. The weakening of residual flows during neap tides suggests a modulation of the net exchange by tidal forcing. This tidal forcing modulation was supported by the weaker stress in neap tides (Fig. 6b) and also by the time series recorded at the shallow channel (distance of 0.75 km in Fig. 6a) where net outflow was identified in the surveys.

The 60-day record of current velocity profiles was low pass-filtered with a Lanczos filter at half-power of 34 h, after aligning the currents with the axis of maximum variance (~50°T counterclockwise). The mean flow profile

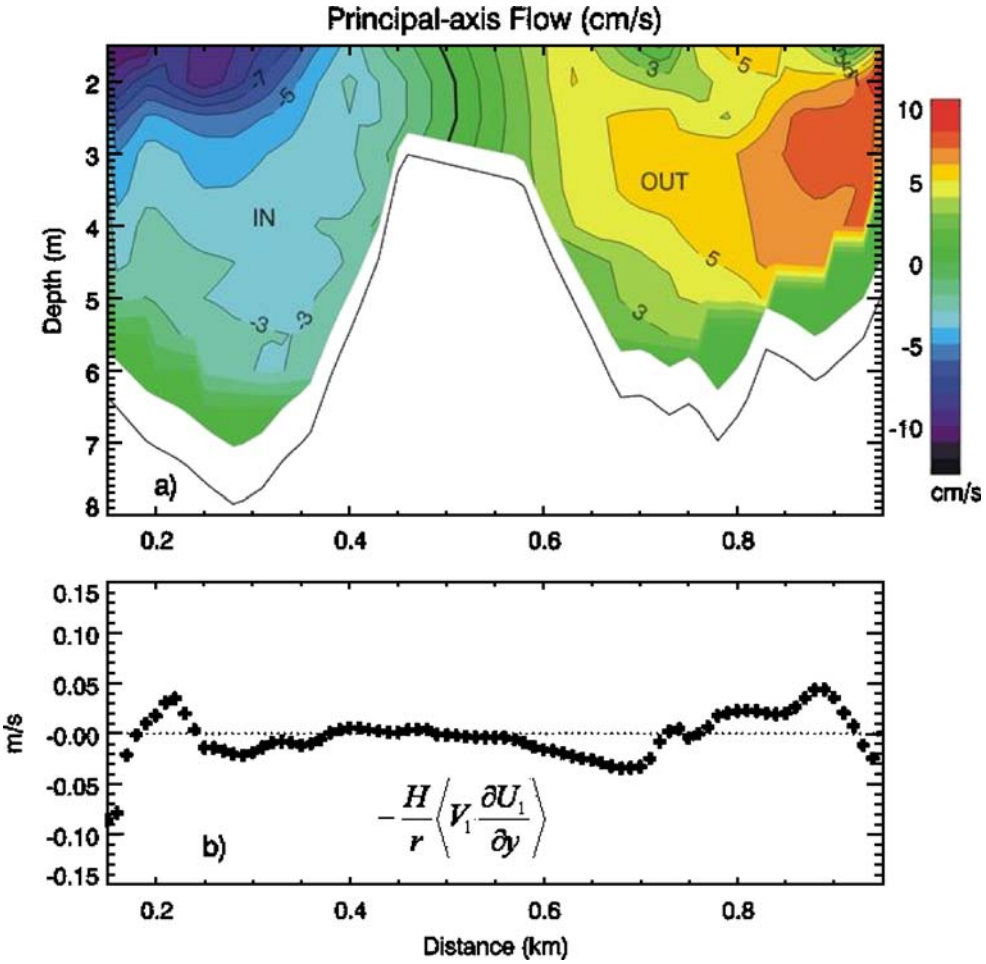

Fig. 5 Same as Fig. 3 but for Ensenada de la Paz during spring tides (looking into lagoon)

during the entire period of observation indicated a net outflow that was only weakly sheared in the vertical direction (upper panel of Fig. 7). This mean flow was modulated mostly by tidal forcing: The strongest outflows were observed during spring tides and the weakest outflows appeared in neap tides (lower panel of Fig. 7). During neap tides with the smallest amplitude (0.4 m), the net outflows were <2 cm/s and increased to ~4 cm/s during the largest spring tides (0.6 m). Such fortnightly modulation was also appreciable throughout the length of the record (Fig. 8, middle panel). The strongest net flows coincided with spring tides and the weakest appeared in neap tides. There were even weak inflows that developed at the surface during neap tides (days 98–99 and 114–155). It is possible that an inverse estuarine circulation developed during these periods of weak tidal forcing because of the net inflows observed near the surface. Wind forcing seems to have had a negligible influence on mean flows (Fig. 8, top two panels), as the net flows did not seem to respond to wind variability. Nonetheless, the predominance of the tidal modulation on mean flows was also clear through normalized energy spectra at each bin recorded by the current profiler (Fig. 9). The spectra show production of several depth-independent overtides (M4—4 cycles per day and M6—6 cycles per day) and compound tides (e.g., MK3—3 cycles per day). The depth uniformity of the spectral amplitudes is a clear indicator of barotropic tidal distortions that result in mean flows (Parker 2007).

The data from San Quintin lagoon show that the mean flow over the observation period in the entrance channel was inward throughout the water column (Fig. 10). This was consistent with the patterns of net inflow in the channel for short channels, as described above. The record at each ADCP bin was low-pass filtered with a Lanczos filter at half power of 34 h. The subtidal variations of the residual flow displayed an obvious fortnightly modulation (lowest panel in Fig. 10). Wind forcing was insignificant in producing the subtidal variability observed. The strongest net flows appeared in spring tides because of tidal rectification, as with Ensenada de La Paz. The influence of tidal rectification as the main driver of mean flows was also seen in normalized power spectra (Fig. 11a) and in the amplitude of wavelet coefficients (Fig. 11b) derived from the surface bin of the ADCP. The spectra showed evident

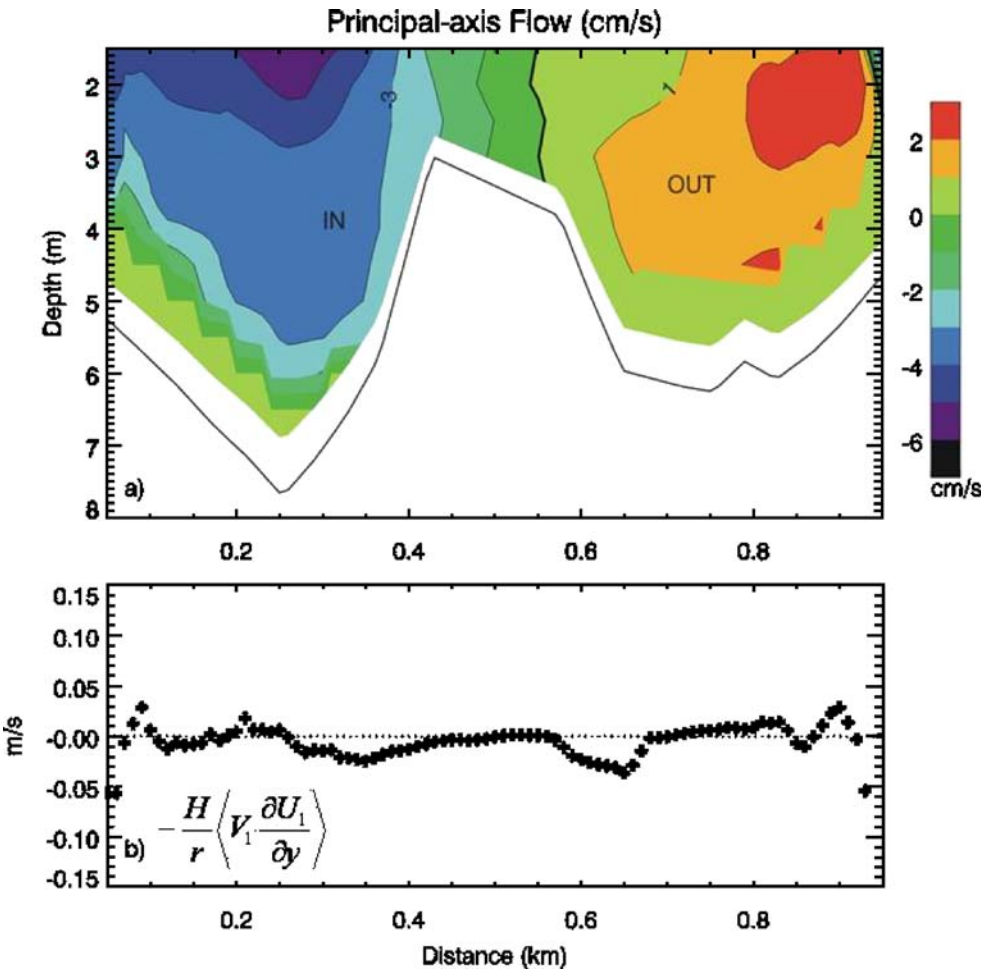

Fig. 6 Same as Fig. 3 but for Ensenada de la Paz during neap tides

generation of depth-independent overtides and compound tides. The amplitude of the distortions, illustrated by the wavelet coefficients, increased in spring tides and decreased in neap tides. Therefore, greater tidal distortion during spring tides translated into stronger tidal residuals than in neaps. A similar tidally induced pattern as those discussed above for standing tidal waves was also observed in Laguna San Ignacio (Winant and Gutierrez de Velasco 2003), a few hundred kilometers to the south of San Quintin Bay. Furthermore, a similar tidal modulation of shallow water constituents like that found in San Quintin Bay was observed in Yavaros Bay (Dworak and Gomes-Valdes 2005), across the Gulf of California on mainland Mexico.

Discussion

There are two noteworthy issues related to the exchange patterns described above that merit more discussion. One issue is related to the pattern of tidally induced exchange flows that resembles that of wind-driven flows and density-driven flows. The other issue is related to the fact that the observations presented in this paper illustrate the net exchange pattern that develops only in short systems, where the tidal elevation and currents are in quadrature. With respect to the first issue, the tidally driven exchange pattern illustrated in this paper is consistent with that of density-driven flows under strong frictional influences (Wong 2004). However, an important distinction between density-driven and tidally induced flows is that their modulation is opposite. In density-driven flows, stronger exchange develops in neap tides (e.g., Haas 1977; Nunes and Lennon 1987) than in spring tides. However, in tidally driven flows, stronger exchange appears in spring tides as discussed in this paper. There are estuaries where these opposite modulations compete to determine the net flows (e.g., Li et al. 1998). Furthermore, wind-driven flows over lateral bathymetric variations consisting of a channel flanked by shoals display downwind flow over the shoals and upwind flow in the channel (e.g., Wong 2004; Winant 2004). Thus, for up-estuary winds, the wind-driven exchange flow should compete against the tidally induced residual flow in short basins and should result in weak exchange flows. On the other hand, for down-estuary winds,

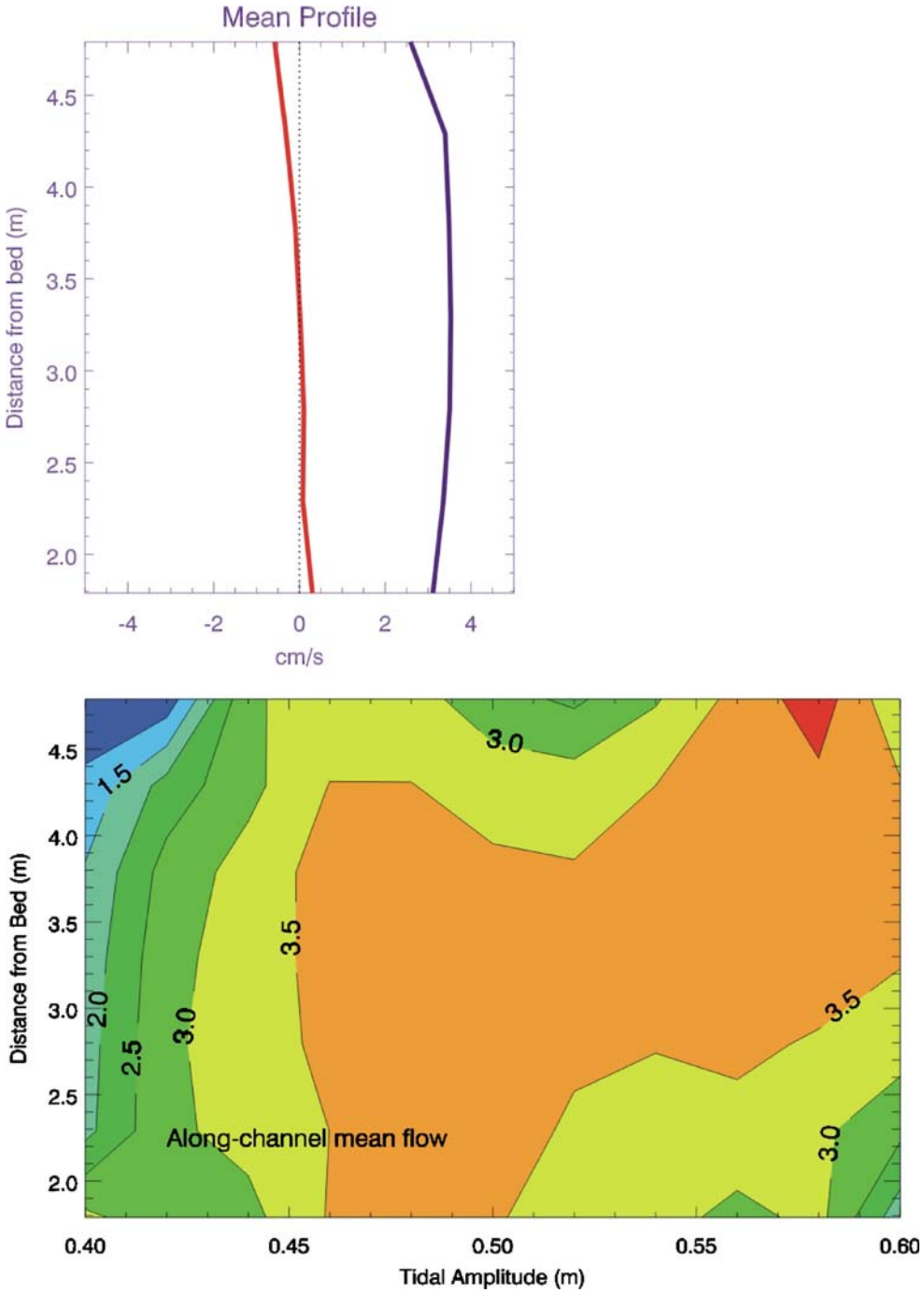

Fig. 7 Mean flow profile throughout the 60-day deployment in Ensenada de La Paz (*upper panel*) and along-channel mean flow profile (cm/s) as a function of tidal amplitude (*lower panel*). In the *upper panel*, the *blue line* is the along-channel component and the *red line* is the cross-channel component

the wind-driven exchange flow should reinforce the tidally driven exchange flow in short basins.

The second issue of the discussion refers to the fact that only the exchange pattern that develops from standing waves, i.e., in short systems, is illustrated in this paper with observations (Table 1). The Stokes term calculated with the time series at Ensenada de la Paz and San Quintin Bay, the two semiarid sites where time series are available, yields residual velocities of only a few millimeters per second, at spring tides. Neap tides yield values <1 mm/s. Throughout the time series, the flow and sea level remain in near-quadrature (<10°), rendering rather small covariances between sea level and flow. Furthermore, all of the cross-sections are less than 1 km wide, and the maximum phase lags for tidal flows from shoals to channel are <10 min. In wider cross-sections, there will indeed be larger phase lags, and the Stokes term may then display lateral variability and become important at some locations of the section. This is a

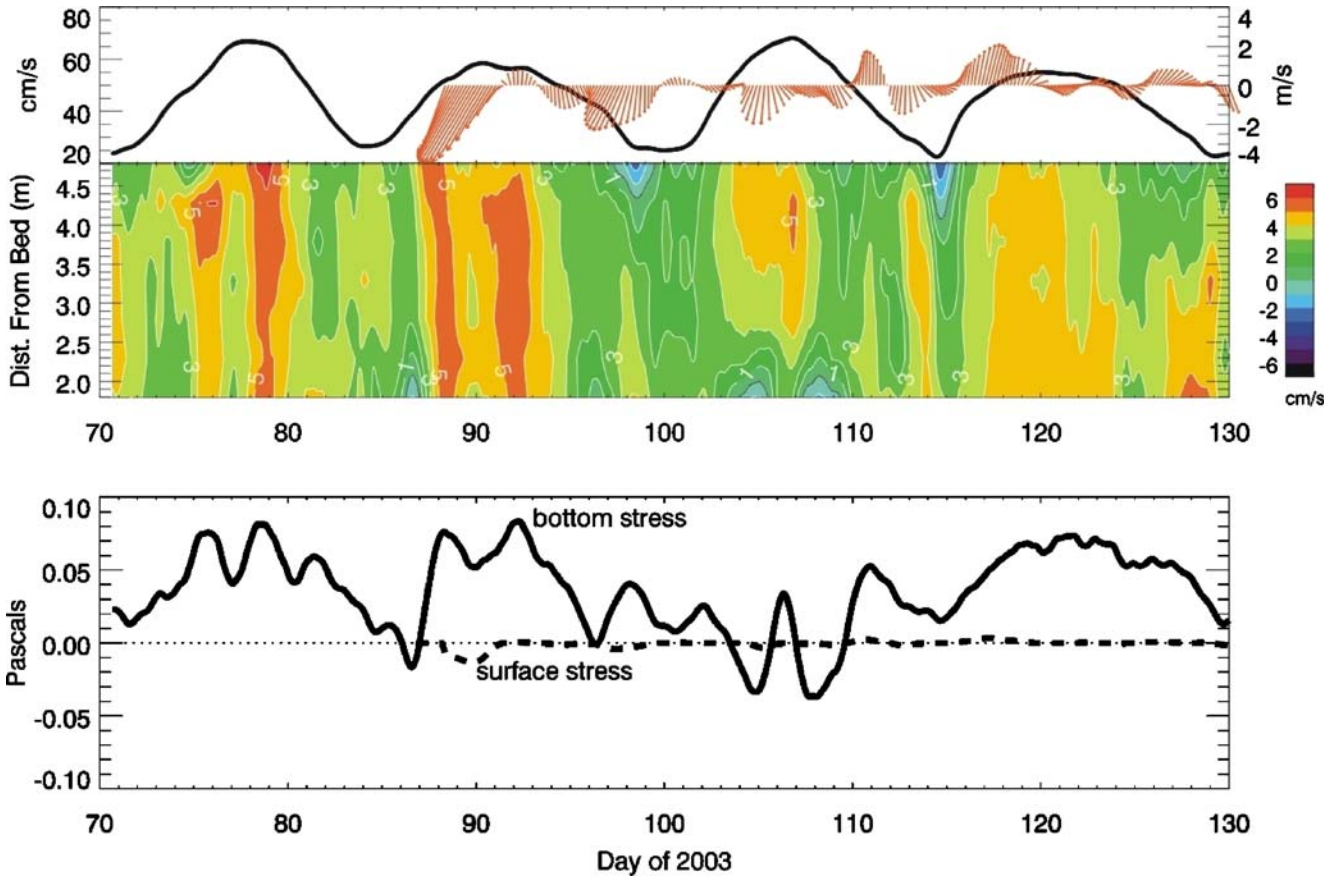

Fig. 8 *Upper panel* shows the time series of low-pass filtered along-channel flow profiles in Ensenada de La Paz (*colored contours*), together with the tidal current amplitude (cm/s, *black line*) and wind velocity (*red vectors*, oceanographic convention). The *lower panel* shows the time series of bottom stress (*continuous line*) and surface (wind) stress during the deployment period

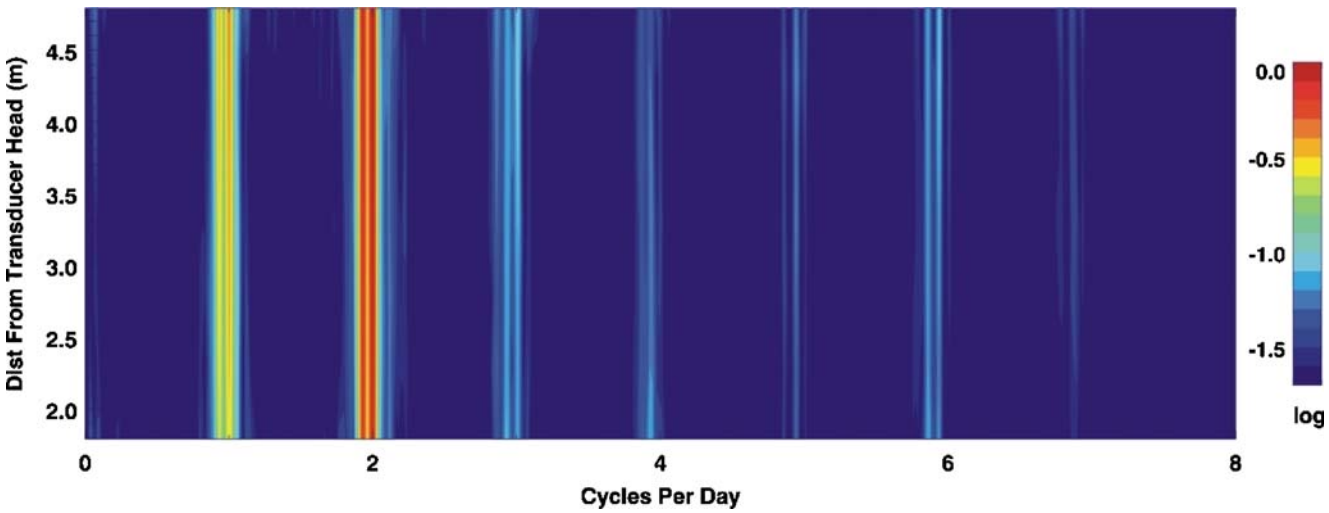

Fig. 9 Logarithm of the normalized power spectrum for the different bins of the ADCP record of Ensenada de la Paz. The most energetic signals are from semidiurnal (two cycles per day—cpd) and diurnal (1 cpd) constituents. Various overtides (4 and 6 cpd) and compound tides (3, 5, and 7 cpd) are apparent

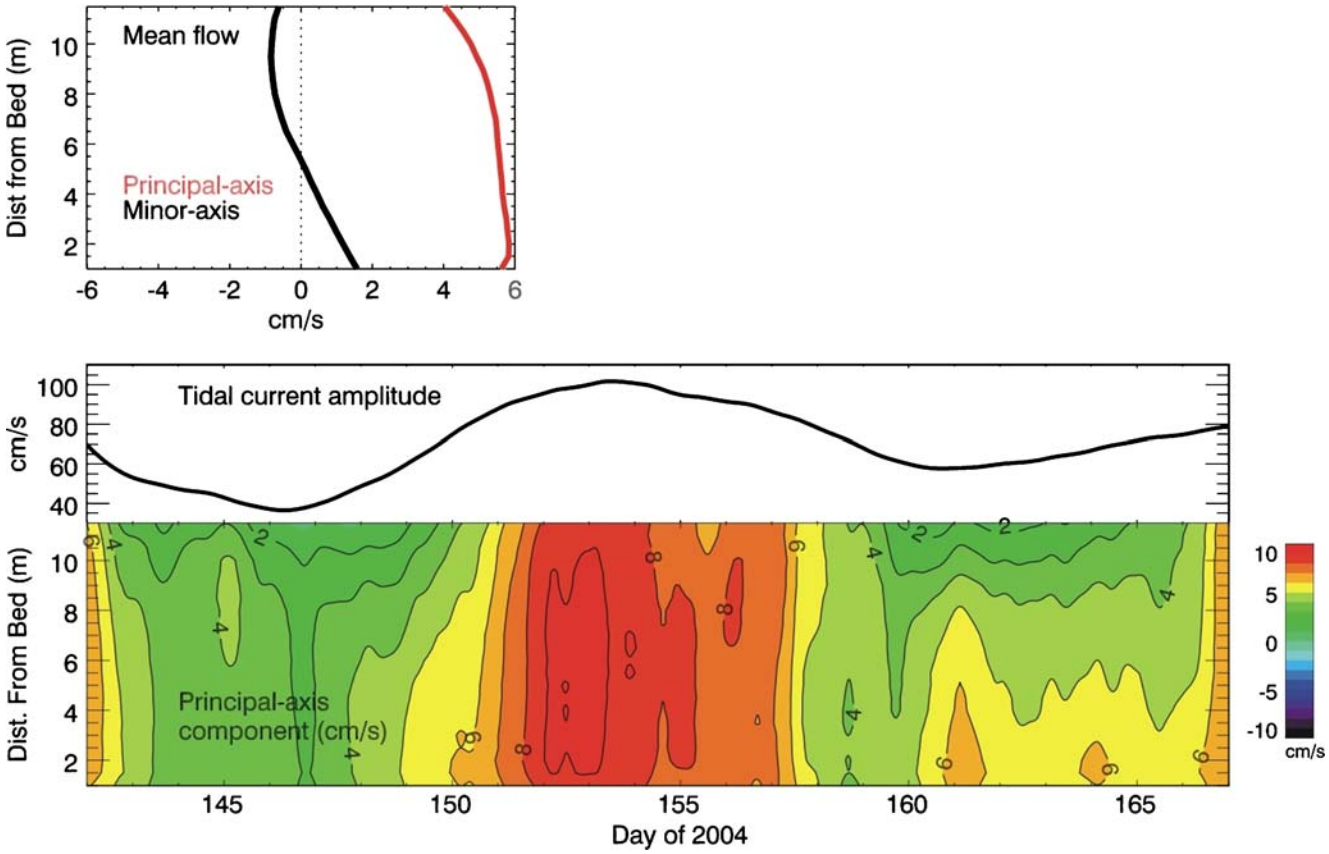

Fig. 10 Mean flows throughout deployment at San Quintin Bay (*upper panel*). Low-pass filtered along-channel flow profiles (*colored contours*), together with the tidal current amplitude (cm/s, *black line*) (*lower panels*). Positive flows denote inflow

topic worth exploring in wider lagoons. In progressive waves, where the basin is longer, the Stokes transport becomes relevant, and the exchange pattern at the basin's entrance reverses. Even though there are no examples presented in this paper, there have been observations in the Chilean Inland Sea, in Canal Chacao (Cáceres et al. 2003), and in North Inlet, South Carolina (Kjerfve and Proehl 1979) that show outflow in the channel and inflow over shoals. In Canal Chacao, the tide is progressive, tidal currents exceed 3 m/s, the water column is mixed, and the mean flows are tidally driven. In addition,, in Ponce de Leon Inlet, on the east coast of Florida, the tide is between progressive and standing (Waterhouse and Valle-Levinson, in preparation), and the net exchange flow consists of outflow in the channel and inflow over the shoals. In that inlet, the baroclinic pressure gradients are negligible relative to the tidal stress. Furthermore, the exchange flow seems to be generally modulated by remote forcing, except that tidal residuals strengthen during the largest spring tides of the month.

It should be mentioned that all the lagoons examined have intricate morphology, indeed, and may not be appropriate for comparison with the theories of Li and O'Donnell (2005) and Winant (2008). In particular, St. Augustine and Jupiter inlets are connected to Florida's Intracoastal Waterway, which complicates the tidal behavior in the area and hinders any validation of theoretical results. Nonetheless, it can be said that the observed exchange flow at the entrance to all lagoons was driven by tidal rectification and its pattern was consistent with theoretical results.

Conclusions

This study presents observational evidence that supports theoretical results of tidally driven exchange patterns in short basins where the tide is a standing wave, i.e., where the tidal elevation and currents are in quadrature. This pattern consists of net inflow in the channel and net outflow over the adjacent shoals and is modulated by tidal forcing. Stronger net exchange flows develop during spring tides relative to neap tides. The tidal modulation on net exchange flows is implicit from theoretical models but is explicitly demonstrated in this study. Furthermore, the modulation is the reverse of what happens in temperate estuaries where density-induced flows dominate over tidal residuals, resulting in relatively stronger net flows in neap tides because of

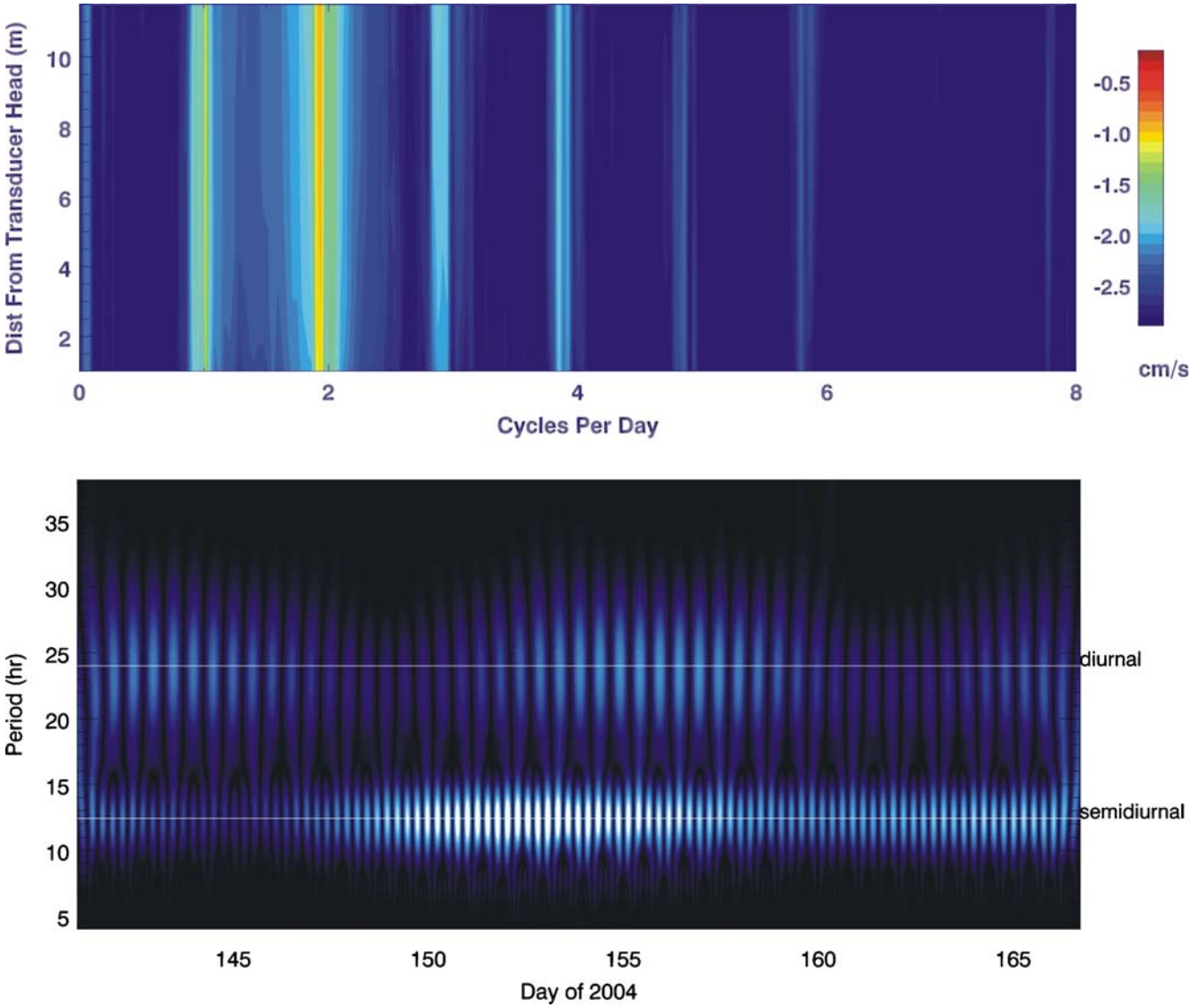

Fig. 11 *Upper panel* Same as Fig. 9 but for San Quintin Bay. *Lower panel* Morlet wavelet coefficients (arbitrary units) for the surface bin of the San Quintin Bay record. Spring tides occur on days 153–154 and 168

reduced vertical mixing. Therefore, subtropical estuaries can be expected to exhibit different net exchange patterns than those observed in temperate estuaries or in systems driven mainly by freshwater input (density gradients).

Acknowledgments The comments of M. Stacey, C. Winant, and A. Waterhouse are gratefully appreciated and helped in the presentation. We thank the efforts of H., Torres, M.A. Cosio, and E. Gonzalez during the data collection in Ensenada de la Paz; of V. Adams, S. Schofield, H. Caliskan, and J. Marin during the data collection in Saint Augustine and Jupiter inlets, and of V. Camacho and A. Mejia in San Quintin Bay. Support for the work at Jupiter Inlet was made possible by funding from the Jupiter Inlet District, Michael Grella Executive Director. AVL acknowledges support from NSF projects OCE-0551923 and OCE-0726697. The support from the Mexican Commission on Science and Technology (CONACYT) for the San Quintin data collection, under project D40144F, is appreciated.

References

Cáceres, M., A. Valle-Levinson, and L. Atkinson. 2003. Observations of cross-channel structure of flow in an energetic tidal channel. *Journal of Geophysical Research* 108C4: 3114. doi:10.1029/2001JC000968.

Dworak, J.A., and J. Gomez-Valdes. 2005. Modulation of shallow water tides in an inlet-basin system with a mixed tidal regime. *Journal of Geophysical Research* 110: C01007. doi:10.1029/2003JC001865.

Geyer, W.R., J.H. Trowbridge, and M.M. Bowen. 2000. The dynamics of a partially mixed estuary. *Journal of Physical Oceanography* 30: 2035–2048. doi:10.1175/1520-0485(2000)030<2035:TDOAPM>2.0.CO;2.

Haas, L.W. 1977. The effect of the spring-neap tidal cycle on the vertical salinity structure of the James, York and Rappahannock Rivers, Virginia, U.S.A. *Estuarine and Coastal Marine Science* 5: 485–496. doi:10.1016/0302-3524(77)90096-2.

Kjerfve, B., and J.A. Proehl. 1979. Velocity variability in a cross-section of a well mixed estuary. *Journal of Marine Research* 37: 409–418.

Li, C.Y., and J. O'Donnell. 2005. The effect of channel length on the residual circulation in tidally dominated channels. *Journal of Physical Oceanography* 35: 1826–1840. doi:10.1175/JPO2804.1.

Li, C.Y., A. Valle-Levinson, K.C. Wong, and K.M.M. Lwiza. 1998. Separating baroclinic flow from tidally induced flow in estuaries. *Journal of Geophysical Research* 103C5: 10,405–10,417. doi:10.1029/98JC00582.

Nihoul, J.C.J., and F.C. Ronday. 1975. The influence of the tidal stress on the residual circulation. *Tellus* 27: 484–489.

Nunes, R.A., and G.W. Lennon. 1987. Episodic stratification and gravity currents in a marine environment of modulated turbulence. *Journal of Geophysical Research* 92C5: 5465–5480. doi:10.1029/JC092iC05p05465.

Parker, B. 2007. Tidal analysis and prediction,. NOAA Special Publication NOS CO-OPS 3, 378.

Pinet, P.R. 2006. *Invitation to oceanography*, 4th Edition. Sudbury, MA, USA: Jones & Bartlett Publishers, Inc., 594 pp.

Pingree, R.D., and L. Maddock. 1977. Tidal residuals in the English Channel. *Journal of the Marine Biological Association of the United Kingdom* 57: 339–354.

Robinson, I.S. 1981. Tidal vorticity and residual circulation. *Deep Sea Research* 28A3: 195–212.

Valle-Levinson, A. 2008. Density-driven exchange flow in terms of the Kelvin and Ekman numbers. *Journal of Geophysical Research* 113: C04001. doi:10.1029/ 2007JC004144.

Valle-Levinson, A., and L. Atkinson. 1999. Spatial gradients in the flow over an estuarine channel. *Estuaries* 222A: 179–193.

Webb, B.M., J.N. King, B. Tutak, and A. Valle-Levinson. 2007. Flow structure at a trifurcation near a North Florida inlet. *Continental Shelf Research* 27: 1528–1547. doi:10.1016/j.csr.2007.01.021.

Winant, C.D. 2004. Three-dimensional wind-driven flow in an elongated, rotating basin. *Journal of Physical Oceanography* 34: 462–476.

Winant, C.D. 2008. Three dimensional residual tidal circulation in an elongated, rotating, basin. *Journal of Physical Oceanography* 38: 1278–1295.

Winant, C.D., and G. Gutiérrez de Velasco. 2003. Tidal dynamics and residual circulation in a well-mixed inverse estuary. *Journal of Physical Oceanography* 33: 1365–1379.

Wong, K.-C. 2004. On the nature of transverse variability in a coastal plain estuary. *Journal of Geophysical Research* 99C7: 14,209–14,222.

Zimmerman, J.T.F. 1978. Topographic generation of residual circulation by oscillatory (tidal) currents. *Geophysical and Astrophysical Fluid Dynamics* 11: 35–47.